Modeling Analysis of Membrane Reactor for Biodiesel Production

Mei Fong Chong
R&D Center for Membrane Technology and Dept. of Chemical Engineering, Chung-Yuan Christian University, Chung-Li, Taiwan 320, R.O.C.
Dept. of Chemical and Environmental Engineering, Faculty of Engineering, The University of Nottingham, Jalan Broga, 43500, Semenyih, Selangor, Malaysia

Junghui Chen
R&D Center for Membrane Technology and Dept. of Chemical Engineering, Chung-Yuan Christian University, Chung-Li, Taiwan 320, R.O.C.

Pin Pin Oh
Dept. of Chemical and Environmental Engineering, Faculty of Engineering, The University of Nottingham, Jalan Broga, 43500, Semenyih, Selangor, Malaysia

Zong-Sheng Chen
R&D Center for Membrane Technology and Dept. of Chemical Engineering, Chung-Yuan Christian University, Chung-Li, Taiwan 320, R.O.C.

DOI 10.1002/aic.13809
Published online May 22, 2012 in Wiley Online Library (wileyonlinelibrary.com).

Recently, membrane reactor technology was used to produce high-quality biodiesel because of its advantage of simultaneous transesterification and separation. As the transesterification reaction involves two immiscible phases of methanol (MeOH) and oil (TG), a thorough investigation on the membrane reactor for biodiesel production with the consideration of chemical phase equilibrium (CPE) via modeling analysis, was conducted in this study. A mathematical model was developed based on the modified Maxwell-Stefan model with the incorporation of CPE. The formation of TG rich micelles dispersed in the continuous phase of MeOH was the most important hypothesis in the model development. The preliminary experiment results show that the permeate compositions from the membrane reactor were closely related to CPE of the system, which was highly depending on the MeOH to TG molar ratio. TG free permeate can only be obtained if the continuous phase of MeOH was free from TG and the TG rich micelles were retained by the membrane. The model verification further confirmed the formation of micelles dispersed in the continuous MeOH phase within the feed side of the membrane reactor and the model was able to predict the performance of the membrane reactor for biodiesel production at an acceptable accuracy. © 2012 American Institute of Chemical Engineers *AIChE J,* 59: 258–271, 2013
Keywords: biodiesel, chemical phase equilibrium, membrane reactor, Stefan-Maxwell model, transesterification

Introduction

Biodiesel attracted tremendous attention during the past decade as a renewable and environmental friendly fuel due to its clean-burning character with fewer emissions of carbon monoxide, sulfur compounds, particulate matter and unburned hydrocarbons. The most common commercial way to produce biodiesel is by transesterification, which refers to a catalyzed chemical reaction between alcohol and triglyceride (TG) to yield fatty acid ester (FAE) and glycerol where the alkali-catalyzed transesterification is more commercially preferred.[1]

The major technical challenge in biodiesel production is the heterogeneity of the system, causing a mass-transfer limited transesterification.[2,3] One of the approaches to overcome this problem is to create a homogeneous reaction mixture by using a cosolvent[4,5] or supercritical methanol,[6] which is costly. In addition, the unreacted materials retained in the biodiesel product and the reversible nature of transesterification caused the needs of further purification to meet the stringent standard of commercial biodiesel, which requires high purity. The ASTM D 6751 standard for biodiesel allows only 0.24% of total glycerol in the final product, implying that high-reaction conversion of 99.7% is required to meet the stated purity.[7] Alternatively, multiple washing steps of the product stream are usually employed to separate and purify the biodiesel, which cause a waste treatment problem.

Recently, two-phase membrane reactor technology for simultaneous transesterification and separation to produce high-quality biodiesel has received attention to overcome the aforementioned problems.[1,7,8,9] The continuous separation of

Correspondence concerning this article should be addressed to J. Chen at Jason@wavenet.cycu.edu.tw

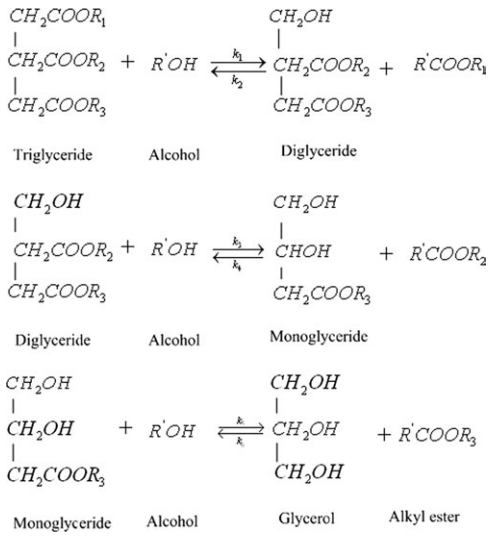

Figure 1. Elementary reaction scheme for the transesterification of TG.

byproducts from the reaction mixture in the membrane reactor promotes transesterification to form biodiesel at higher rates.[10] Therefore, the idea of using the membrane reactor is to remove the FAE, glycerol, methanol and catalyst from TG simultaneously so that the reaction will shift toward the favorable path. To achieve successful operation of the membrane reactor, a pseudo homogeneous reaction to achieve high conversion and heterogeneous separation to obtain high purity of biodiesel, which is free from TG, must be obtained. The results obtained by several researchers show an inconsistency for the existence of bonded glycerides in the permeate stream.[7,10] The inconsistency of the results obtained is due to the heterogeneity of the reacting mixture in the feed side of the membrane reactor which can be explained by the chemical phase equilibrium (CPE) of the system. Hence, the knowledge of chemical phase behavior of the multicomponent system in biodiesel production is very important to achieve the optimum and consistent performance.

Cheng et al.[9] shows that liquid-liquid equilibrium (LLE) is the key factor to ensure the desired separations are achieved. The results showed that TG-free permeate stream with high-permeation rate was achieved when the feed bulk composition of TG-FAE-alcohol was controlled within the two-phase zone of the system. Although the LLE for TG-FAE-alcohol has been investigated by Cheng et al.[9] the investigation on ternary phase equilibrium alone without considering the reaction cum phase equilibrium was inadequate to define the six-component biodiesel production system. In addition, the effects of transesterification reaction with changing compositions within the CPE cause the system to be more complicated and difficult to be controlled within the desired composition/phase zone.

Unfortunately, mathematical models suitable for multicomponent liquid-liquid two-phase membrane reactor for biodiesel production are not available. Modeling a two-phase membrane reactor for biodiesel production is very important to describe, investigate and optimize the simultaneous transesterification and separation efficiencies. Therefore, the ultimate goal in this study is to conduct a thorough investigation for the first time on the membrane reactor for biodiesel production with the consideration of LLE or to be more precisely, CPE via modeling analysis.

This research was conducted with three parts. The first part focused on the hypothesis and mathematical model development based on the modified Maxwell-Stefan model with the incorporation of CPE. The basic phenomenon of transesterification reaction which permits the simultaneous reaction and separation in the membrane reactor was carefully outlined to form the hypothesis, framework and boundary for model development. It was then followed by model development which consisted of the consideration of CPE effects at the feed side of the membrane, intramembrane and gel polarization layer mass transports.

In the second part of this study, a preliminary experimental analysis was conducted to investigate the effects of CPE on the membrane separation efficiency by isolating the effects of reaction by using a batch reactor to obtain a constant equilibrated mixture for membrane separation. The preliminary experimental results were then used to validate the basis and hypothesis of the model proposed besides highlighting the importance of modeling analysis in this study. In the final part of the study, the model was solved by using regression with the experimental data obtained from the preliminary experiment. The model was validated by comparing the simulated results with the experimental results based on the coefficients of determination (R^2) value.

Basis of the Membrane Reactor for Biodiesel Production

Membrane reactor is a devise used for carrying out a reaction and a membrane-based separation simultaneously in the same physical enclosure.[7] In this study, a membrane reactor using ultrafiltration to produce biodiesel at high purity from canola oil via alkali-catalyzed methanolysis was considered for the development of the mass-transport model. The main component of biodiesel in this case, fatty acid methyl ester (FAME) was the product of transesterification of lipids (TG) by using straight-chain alcohol (methanol or MeOH) which was catalyzed by sodium hydroxide (NaOH). Transesterification of TG consists of three reaction steps, which are depicted in Figure 1.[11]

The basis of the membrane reactor operation for biodiesel production can be explained with the aid of Figure 2. The membrane reactor is operated in an isothermal condition controlled at the temperature near to the boiling point of MeOH (e.g., 333 K) and it has a cross flow velocity u_t adequate for mixing. As the MeOH and TG are immiscible, the mixture in phase equilibrium will form a biphasic system with MeOH rich phase (polar phase) and TG rich phase (nonpolar phase).[10] To ensure a pseudo-homogeneous reaction and heterogeneous separation, efficient mixing is needed to form an emulsion (1) to promote mass transfer between MeOH rich phase and TG rich phase for effective reaction, and (2) to obtain oil droplets/micelles of TG rich phase so that TG can be retained in the retentate side of the membrane reactor due to their bigger particle size than the membrane pore size. The formation of monoglyceride (MG) and

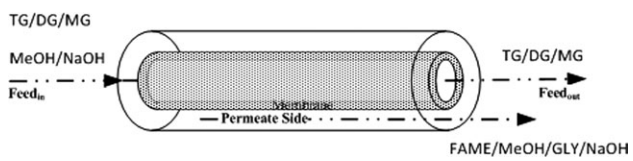

Figure 2. Transesterification of Canola oil using tubular membrane reactor.

diglyceride (DG), which are the surfactants, is also important to promote the formation of emulsion.

The formation of emulsion with dispersed oil droplets/micelles in the continuous MeOH rich phase will allow efficient transesterification at the surface of the oil droplets suspended in the MeOH.[1] Both the products of transesterification, namely, FAME or biodiesel and glycerol (Gly) are then diffused from the oil droplets and dissolved in the MeOH rich phase. This is the physical characteristic which permits the membrane reactor to separate FAME from TG. The FAME/MeOH/Gly/NaOH phase will then pass through the membrane into the permeate stream.[1] In an ideal condition, the permeate stream of FAME/MeOH/Gly/NaOH will form a single phase at 333 K as a clear, amber and homogeneous solution. The permeate will de-phase immediately into a biphasic system which consists of FAME rich phase and Gly rich phase when it is cooled to room temperature.[7] However, at certain occasions, trace amount of DG and MG will permeate through the membrane pores. Even so, MG is unstable and will be transesterified to FAME rapidly with this of MeOH and NaOH in the permeate stream. Thus, this could be the most reasonable explanation on only trace amount of DG, but neither TG nor MG can be found in the permeate stream.[7] The permeation of DG into the permeate stream could be attributed by:

1. Residue in the hydrophobic oil droplets/micelles, where the oil droplets/micelles could have particle size smaller than the membrane pore size.
2. Solubilized in the continuous FAME - MeOH rich phase.

Model Development

Consider a membrane reactor which is continuously fed with a mixture of MeOH and TG with alkali-catalyst (NaOH). The MeOH:TG ratio at the feed side is controlled so that MeOH becomes the continuous phase, and transesterification occurs at the surface of oil droplets formed due to efficient mixing. Once the transesterification occurs, the FAME/Gly/NaOH solubilized in MeOH rich phase with trace amount of TG, DG and MG will permeate through the membrane as shown in Figure 3. The MG will further react to form FAME in the permeate stream. As the oil droplets are too large to pass through the membrane pores, they will be retained on the membrane wall forming a polarized layer, which poses the major mass transfer limitation for permeation. Thus, the permeation of mobile phase of FAME - MeOH rich phase is governed by its equilibrium with the TG rich phase at the membrane interface instead of the membrane material itself. This is the first assumption made for the transport of a biphasic system through a membrane and is illustrated in Figure 3. The components are then taken as the concentrations, C_i^I in the mobile FAME - MeOH rich phase, whereas the TG rich phase is considered as a single component dispersed as micelles in the FAME - MeOH rich phase. By defining the FAME - MeOH rich phase as *Phase I* and TG rich phase as *Phase II*, the components *i* in *Phase I* written in terms of concentrations in the membrane reactor consist of MeOH, FAME, Gly, TG, MG, DG and oil droplets/micelles, in which the superscript *I*, shows the solute concentrations are taken at *Phase I*. Similarly, the *Phase II* will also consist of MeOH, FAME, Gly, TG, MG and DG, which can be written in terms of concentrations as C_i^{II} and the summation of these concentrations will lead to the oil droplets/micelles concentration $C_{Micelle}^I$. The superscript *II*

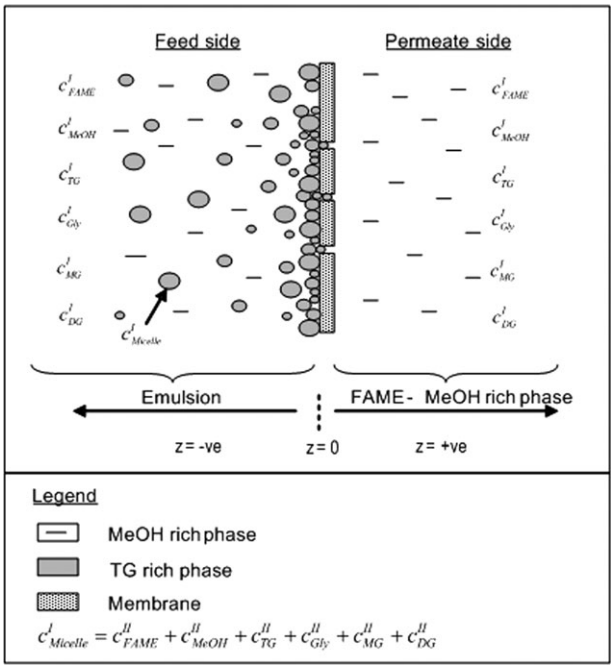

Figure 3. Schematic diagram of membrane reactor for biodiesel production.

shows the solute concentrations of *Phase II*. Therefore, the membrane reactor involves multicomponent separations by assuming the alkali-catalyst to be negligible. As excess of MeOH is used to ensure the MeOH becomes the continuous phase, MeOH is regarded as solvent and other components are regarded as solute.

Intramembrane mass transport for two-phase liquid system

For a system in which no body forces (e.g., gravity, electrical) are present, the one-dimensional (1-D) transport in a membrane by considering cylindrical pores can be described by Maxwell-Stefan equation as[12]

$$\frac{x_i}{RT}\nabla_{T,P}\mu + \frac{C_i\overline{V}_i}{C_tRT}\nabla P = \sum_{j=1}^{n}\frac{x_iN_j - x_jN_i}{C_tD_{ij}} - \frac{1}{B_o}\kappa_i\Phi_iu_i \quad (1)$$

The term x is the mole fraction, R is the gas constant, T is temperature, $\nabla_{T,P}\mu$ is the chemical potential gradient, C is the molar concentration, $\overline{V}$ is the specific molar volume, ∇P is the pressure gradient, N is the solute flux, D is the Maxwell-Stefan diffusion coefficient, B_o is the permeability parameter, κ is fractional viscosity coefficient, Φ is the volume fraction, and u is the velocity. Both subscripts and indicate for individual solute condition, whereas t indicates total solute conditions.

The first term denotes the driving force due to chemical potential gradient, assuming interactions only occur in the solution itself at constant temperature and pressure. The pressure effects created when the solute molecules collide with the wall of the pore are not taken into account as the permeation of liquids for which the mean free path is much smaller than the pore diameter. The second term denotes the driving force due to the hydrodynamic pressure gradient developed within the membrane layer. This term is derived by the introduction of the membrane as a separate component and the "clamping" force to keep the membrane in place.[12]

By looking at the feed side of the membrane reactor, the components are considered in equilibrium with MeOH and TG rich phases. Thus, for the system consists of n solutes in a solvent, as $i = 1, 2, 3.....n$ and $i = 1$ for TG rich micelles, the 1-D transport in membrane as in the Maxwell-Stefan equation (Eq. 1) describing the fluxes per unit membrane area in Fickian form, which takes into the consideration of membrane porosity, ε and tortuosity, τ can be written as[12]

$$N = -[S]\frac{\partial C}{\partial z} + u^v[K_v]\,C \tag{2}$$

The superscript I, is omitted in Eq. 2 since all the solute concentrations are taken with the reference of *Phase I*. u^v is the volume-averaged velocity (or volumetric flux), and z is the distance coordinate perpendicular to the membrane surface (see Figure 3). The convective friction matrix $[K_v]$, can be taken as

$$[K_v] = [G]^{-1}[F] \tag{3}$$

where the convective part $[F]$, and generalized friction matrices [G], are represented as

$$\begin{aligned}
[F]_{ij} &= \frac{\tau}{\varepsilon}\delta_{ij}\left(\frac{(C_t)^2\overline{V_i}\,\overline{V_n}}{B_o}\kappa_n + \frac{1}{D_{in}}\right)\\
[G]_{ij} &= \frac{\tau}{\varepsilon}[B]_{ij} + \frac{\tau}{\varepsilon}\left(\delta_{ij}\frac{\kappa_i C_t\overline{V_i}}{B_o} - \frac{C_t\Phi_i}{B_o}\left(\kappa_j\overline{V_j} - \kappa_i\overline{V_i}\right)\right)\\
[B]_{ii} &= \frac{1}{C_t}\left[\frac{\Phi_i}{\overline{V}_t D_{in}} + \sum_{\substack{k=1\\k\neq i}}^{n}\frac{\Phi_k}{\overline{V}_k D_{ik}}\right]\\
[B]_{ij} &= -\frac{\Phi_i}{\overline{V}_i C_t}\left[\frac{1}{D_{ij}} - \frac{1}{D_{in}}\right];\quad i \neq j
\end{aligned} \tag{4}$$

where δ_{ij} is the Kronecker delta. The value of κ_i in the generalized friction matrix $[G]$, and convective part matrix $[F]$ for multicomponent system can be approximated to steric exclusion coefficient as[13]

$$\kappa_i = \left(1 - \frac{d_{\text{solute}}}{d_{\text{pore}}}\right)^2 \tag{5}$$

with d_{solute} and d_{pore} as solute and pore diameter, respectively. The average droplets/micelles size of d_{solute} can be estimated from simplified correlation equations based of two-dimensionless (2-D) parameters.[14,15] The B_o is estimated by assuming cylindrical pore of radius r_{pore}[16]

$$B_o = \frac{r_{\text{pore}}^2}{8} \tag{6}$$

In Eq. 2, the volume-averaged velocity u^v can be calculated as[17]

$$u^v = L_P\Delta P_{\text{flow}} = L_P(\Delta P_{\text{total}} - \sigma\,\Delta\Pi) \tag{7}$$

The driving force term $\Delta P_{\text{flow}} = \Delta P_{\text{total}} - \sigma\,\Delta\Pi$ is the ratio of volume-averaged velocity, u^v to hydraulic permeability constant L_p.[12] ΔP_{total} is the total pressure difference of the system or trans membrane pressure, $\Delta\Pi$ is the osmostic pressure difference across the membrane, dependant on the concentrations on both sides, and σ is the osmostic reflection coefficient. The osmostic pressure difference across the membrane $\Delta\Pi$, is given as[12,17]

$$\begin{aligned}
\Delta\Pi = RT\sum_{i=1}^{n}\frac{1}{\overline{\overline{V}}_i}&\left(\ln\gamma_{\delta_{pol},i} + \ln C_{\delta_{pol},i} - \ln C_{\delta_{pol},t}\right)\\
&-\frac{1}{\overline{\overline{V}}_i}\left(\ln\gamma_{p,i} + \ln C_{p,i} - \ln C_{p,t}\right)
\end{aligned} \tag{8}$$

where

$$\gamma_{\delta_{pol},i} = \begin{cases}\bar{\gamma}^{II}_{\delta_{pol},i}; & i = 1\\ \gamma^{I}_{\delta_{pol},i}; & i \neq 1\end{cases};\qquad \gamma_{p,i} = \begin{cases}\bar{\gamma}^{II}_{p,i}; & i = 1\\ \gamma^{I}_{p,i}; & i \neq 1\end{cases} \tag{9}$$

The subscripts δ_{pol} and p show the conditions are taken at the polarization-membrane interface and the permeate side. The symbol $\bar{\gamma}$ shows the average activity coefficient.

The binary Maxwell-Stefan diffusion coefficient, D_{ij} in a multicomponent system, is given by Taylor and Krishna[18]

$$D_{ij} = \left(D^o_{ij}\right)^{(1+x_j-x_i)/2}\left(D^o_{ji}\right)^{(1+x_i-x_j)/2} \tag{10}$$

where the term $D_{ij}{}^{\circ}$ is the infinite dilution diffusion coefficient of species which is infinitely diluted in species j. The Wilke and Chang equation can be used to predict the $D_{ij}{}^{\circ}$ values as[18]

$$D^o_{ij} = 1.173\times10^{-16}\frac{\left(\Phi_j M_j\right)^{1/2}T}{\eta_j V_i^{0.6}} \tag{11}$$

The term M_j is molar mass of solvent j, η is viscosity and Φ_j is association factor for the solvent (1.9 for methanol and 1.0 for other unassociated solvents). V_i is molar volume of solute i at its normal boiling point, which is given by M and density ρ

$$V = \frac{M}{\rho} \tag{12}$$

In Eq. 2, the Fickian matrix inside the membrane, $[S]$ has to be modified in term of thermodynamic factor when two-phase system is concerned. The chemical potential gradient for a solute i at isothermal condition is given as[19]

$$\partial_T\mu_i = RT\,\partial\ln(a_i) + \overline{V}_i\partial P \tag{13}$$

The subscript T, shows an isothermal operation, and a is the activity term. Let us consider n solutes system which forms an equilibrium "homogeneous" condition with *Phase I*. The chemical potential gradient due to the pressure effects can be neglected, whereas the chemical potential gradient due to the concentrations and the effects of LLE must be considered. Thus, the chemical potential gradient with LLE consideration can be written as

$$\partial_{T,P}\mu_i = \begin{cases}RT\,\partial\ln\left(\bar{a}^{II}_i\right); & i = 1\\ RT\,\partial\ln\left(a^{I}_i\right); & i \neq 1\end{cases} \tag{14}$$

The symbol and are the average activity term in *Phase II* and activity term in *Phase I*, respectively.

Therefore, the chemical potential gradient of solute i in multicomponent system where solute-solute interactions are considered can be taken as[12]

$$\nabla_{T,P}\mu_i = \sum_{j=1}^{n-1} \frac{\partial A_i}{\partial C_j} \nabla_{T,P} C_j \quad \text{where } A_i = \begin{cases} RT\partial \ln\left(\bar{a}_i^{II}\right); & i = 1 \\ RT\partial \ln\left(a_i^{I}\right); & i \neq 1 \end{cases} \tag{15}$$

For the activity term, we may write[12]

$$\ln a_i = \begin{cases} \ln \bar{\gamma}_i^{II} + \ln C_i - \ln C_t; & i = 1 \\ \ln \gamma_i^{I} + \ln C_i - \ln C_t; & i \neq 1 \end{cases} \tag{16}$$

where γ_i^I is the activity coefficient of the solute in *Phase I*. For total concentration, we may write

$$C_t = \sum_{j=1}^{n-1} C_j + \left(1 - \sum_{j=1}^{n-1} C_j \overline{V}_j\right) / \overline{V}_n \tag{17}$$

and, thus

$$\frac{\partial C_t}{\partial C_j} = 1 - \frac{\overline{V}_j}{\overline{V}_n} \tag{18}$$

By combining Eqs. 15–18, the first term of Eq. 1 can now be written as

$$\frac{C_i}{RT}\nabla_{T,P}\mu_i = \begin{cases} C_i \sum_{j=1}^{n-1} \left[\frac{\partial \ln \bar{\gamma}_i^{II}}{\partial C_j^I} + \delta_{ij} - \left(1 - \frac{\overline{V}_j}{\overline{V}_n}\right)\right] \nabla_{T,P} C_j; & i = 1 \\ C_i \sum_{j=1}^{n-1} \left[\frac{\partial \ln \gamma_i^{I}}{\partial C_j^I} + \delta_{ij} - \left(1 - \frac{\overline{V}_j}{\overline{V}_n}\right)\right] \nabla_{T,P} C_j; & i \neq 1 \end{cases} \tag{19}$$

and, thus, the thermodynamic factor matrix $[\Gamma_c]$ can be written as[12]

$$[\Gamma_C]_{ij} = \begin{cases} \delta_{ij} + C_i \frac{\partial \ln \bar{\gamma}_i^{II}}{\partial C_j} - \frac{C_i}{C_t}\left(1 - \frac{\overline{V}_j}{\overline{V}_n}\right); & i = 1 \\ \delta_{ij} + C_i \frac{\partial \ln \gamma_i^{I}}{\partial C_j} - \frac{C_i}{C_t}\left(1 - \frac{\overline{V}_j}{\overline{V}_n}\right); & i \neq 1 \end{cases} \tag{20}$$

The Fickian matrix inside the membrane with the consideration of LLE effects, is finally represented as

$$[S] = [G]^{-1}[\Gamma_c] \tag{21}$$

The boundary conditions of Eq. 2 are represented as

$$z = 0; \qquad (C_i) = \begin{cases} \left(\left[K_{eq}\right]^m\right)^{-1} C_{\delta_{pol}}; & i = 1 \\ \left(\left[K_{eq}\right]^{II}\right)^{-1} C_{\delta_{pol}}; & i \neq 1 \end{cases} \tag{22}$$

$$z = L_m; \qquad N_i^m = u^v C_{p,i}; \quad \left(C_i\right) = \left[K_{eq}\right]^m \left(C_{p,i}\right)$$

in which $C_{\delta_{pol}}$ and $C_{p,i}$ are the polarization-membrane interface and permeate concentrations, respectively. $[K_{eq}]$ is the equilibrium matrix with superscript m and II denote for membrane and *Phase II*, respectively and is given as

$$\left[K_{eq}\right]_{ij} = \delta_{ij} K_{eq,i} \tag{23}$$

Polarization layer transport for two-phase liquid system applied to a tubular membrane

For 1-D transport in the polarization layer, the Fickian-type equations for the flux per unit area of the membrane in concentration terms with two-phase system are[18]

$$N = \left\{[D] + [D]_{\text{turb}}\right\} \frac{\partial C}{\partial z} + u^v C \tag{24}$$

The Fickian molecular diffusion matrix, $[D]$ is given by

$$[D] = ([B])^{-1}[\Gamma_c] \tag{25}$$

and the turbulence diffusivity matrix, $[D]_{\text{turb}}$ is given as

$$[D]_{\text{turb}} = D_{\text{turb}}[I] \tag{26}$$

For the turbulence Fickian diffusivity coefficient D_{turb}, the turbulence Schmidt number, Sc_{turb} is assumed to be near unity[12]

$$Sc_{\text{turb}} = \frac{\nu_{\text{turb}}}{D_{\text{turb}}} \approx 1 \tag{27}$$

By definition, the turbulent kinematic viscosity, ν_{turb} for most situations is given as

$$\frac{\nu_{\text{turb}}}{\nu} = \frac{1}{\partial u^+ / \partial y^+} - 1 \tag{28}$$

and the dimensionless variables are defined as

$$\begin{aligned} y^+ &= y u^* / \nu \\ u^* &= \langle u_t \rangle \sqrt{f/2} \\ u^+ &= u/u^* \end{aligned} \tag{29}$$

The term y is the distance from surface in boundary layer ($d_{\text{tube}}/2 - z$) with d_{tube} is the diameter of the tube y^+, is the dimensionless value of y, ν is the kinematic viscosity, u^* is the modified velocity, u^+ is the dimensionless velocity, and u is the velocity along the boundary layer. The term f is the Fanning friction factor defined by

$$\Delta P_{\text{total}} = 4f \frac{1}{2} \rho \langle u_t \rangle^2 \left(\frac{L_{\text{tube}}}{d_{\text{tube}}}\right) \tag{30}$$

where ρ is the total mass concentration, and L_{tube} is the length of the tube. The bulk velocity along the membrane, can be calculated as

$$\langle u_t \rangle = \frac{Q_F}{n_{\text{tube}} \frac{\pi}{4} d_{\text{tube}}^2} \tag{31}$$

in which Q_F is the volume feed flow rate, and n_{tube} is the number of tubes per membrane module.

For Schmidt number, Sc near unity, the values of y^+ can be taken as $0 < y^+ < 5$. The ν_{turb} can be correlated from Eqs. 27–30 as[18]

$$\frac{v_{\text{turb}}}{v} = C_{\text{vieth}}\left(\frac{f}{2}\right)^{3/2}(y^{+})^{3} \tag{32}$$

$$C_{\text{vieth}} = \left(\frac{2}{9}\pi\sqrt{3}\right)^{3} = 1.768 \tag{33}$$

The boundary conditions for Eq. 24 are given as

$$\begin{aligned} z = 0; \qquad & (C_{\delta_{pol},i}) = \begin{cases} [K_{eq}]^{m} C_{m,i}; & i = 1 \\ [K_{eq}]^{II} C_{m,i}; & i \neq 1 \end{cases} \\ z = -\delta_{pol}; \qquad & C_{-\delta_{pol},i} = C_{b,i} \end{aligned} \tag{34}$$

The subscripts $-\delta_{\text{pol}}$, m and b show the solute concentrations at bulk-polarization interface, inside the membrane and at bulk condition. The thickness of boundary layer δ_{pol}, can be determined by the Sieder and Tate correlation of Sherwood number Sh, Reynold number, Re and Schmidt number, Sc in a tubular ultrafiltration module as[20]

$$Sh = 0.0027\text{Re}^{0.8}Sc^{0.33} \tag{35}$$

$$Sh = \frac{k\, d_{\text{tube}}}{\overline{D}} \tag{36}$$

$$\text{Re} = \frac{\rho\langle u_t\rangle d_{\text{tube}}}{\dot{\eta}} \tag{37}$$

$$Sc = \frac{\dot{\eta}}{\rho\overline{D}} \tag{38}$$

where $\overline{D}$ is the Fickian diffusion coefficient and $\dot{\eta}$ is the dynamic viscosity of the mixture. Once the mass-transfer coefficient, k is calculated from Eq. 36, the value of δ_{pol} can be obtained as[17]

$$k = \frac{\overline{D}}{\delta_{pol}} \tag{39}$$

Phase inversion

The membrane reactor will encounter failure in operation during the event of phase inversion if the TG becomes the continuous phase. The pores of the membrane could be plugged or no separation of the FAME from TG depending on the condition of the phase. The point of phase inversion in a two-phase system can be expressed as[21]

$$\frac{\Phi_{MeOH}}{\Phi_{TG}} = 1.22\left(\frac{\eta^{o}_{MeOH}}{\eta^{o}_{TG}}\right)^{0.29} \tag{40}$$

If the values for the viscosities of pure MeOH, $\eta_{MeOH}{}^{\circ}$ and TG, $\eta_{TG}{}^{\circ}$ at 333 K are substituted into the equation, the volume fraction of MeOH, Φ_{MeOH} to TG, Φ_{TG} ratio is calculated as 0.44. Thus, the MeOH to TG ratio should be maintained at $\Phi_{MeOH}/\Phi_{TG} > 0.44$ to avoid phase inversion, which forms the most important process limitation to the membrane reactor.

Bulk concentrations at the feed side of the membrane reactor via chemical phase equilibrium (CPE) calculations

To obtain the bulk concentrations at the feed side of the membrane, C^{I}_{b} which consists of MeOH, FAME, Gly, TG, MG, DG and oil droplets/micelles as shown in Figure 3, the CPE as a result of transesterification need to be obtained. The transesterification reaction or any other reaction systems should satisfy[22]

$$\sum_{i=1}^{n}\beta_{ij}S_i = 0; \qquad j = 1, 2, ..., m \tag{41}$$

where i and j are the component and reaction indices, respectively; β is the stoichiometric coefficient where it is defined to have positive values for products and negative values for reactants, and S is the chemical species. The reaction equilibrium constants, K_j are then defined by

$$\prod_{i=1}^{n}\left(\gamma^{II}_{i}x^{II}_{i}\right)^{\beta_{ij}} = \prod_{i=1}^{n}\left(\gamma^{I}_{i}x^{I}_{i}\right)^{\beta_{ij}} = K_j \tag{42}$$

The values may be determined as[23]

$$K_j = \exp\left(\frac{-\Delta G^{o}_{j}}{RT}\right) \tag{43}$$

where

$$\Delta G^{o}_{j} = \sum_{i=1}^{n}\beta_{ij}G^{o}_{i} \tag{44}$$

The $G_i{}^{\circ}$ is the standard Gibbs free energy of formation. The material balances for multiple reactions are then given as

$$F_{out,i} = F_{in,i} + \sum_{j=1}^{m}\beta_{ij}\xi_j; \qquad i = 1, 2, ..., n \tag{45}$$

F and ξ are defined as the amount of the species and the extent of reaction, respectively. The subscripts *out* and *in* represent for final and initial, respectively.

The condition of CPE can be represented by flash equations as

$$z_i = \frac{F_{out,i}}{\sum_{i=1}^{n}F_{out,i}} \tag{46}$$

$$z_i = \alpha x^{I}_{i} + (1-\alpha)x^{II}_{i} \tag{47}$$

$$x^{I}_{i} = k_i x^{II}_{i} = \frac{\gamma^{II}_{i}}{\gamma^{I}_{i}}x^{II}_{i} \tag{48}$$

$$\sum_{i=1}^{n}x^{I}_{i} = \sum_{i=1}^{n}x^{II}_{i} = 1 \tag{49}$$

where the symbol z is mole fraction in total system including both phases, α is the mole fraction of *Phase I* in the system, and k is the phase equilibrium ratio.

Model Solution

Chemical phase equilibrium (CPE) calculations

Equations 42–49 can be solved once the values of ξ, $\Delta G_j{}^{\circ}$ and γ are known. The values of and can be calculated from the reaction kinetics data of transesterification by taking the

Table 1. Experimental Results of Canola Oil Transesterification in a Batch Reactor at the Temperature of 333 K

#	Catalyst conc (wt%).	MeOH to TG molar ratio	Conversion (%)	Mixture composition (% wt)					
				MeOH	FAME	Gly	TG	DG	MG
1	0.05	12:01	95.68	20.82	72.01	0.79	4.32	1.17	0.88
2	0.1	12:01	99.00	20.57	72.95	3.77	2.18	0.10	0.43
3	0.5	12:01	~100	18.39	76.09	5.46	ND	ND	0.06
4	0.1	06:01	87.89	4.09	75.98	2.20	12.11	1.55	4.07
5	0.1	18:01	97.56	23.02	71.38	1.80	2.44	0.54	0.82
6	0.1	24:01	91.16	21.43	61.09	5.52	8.84	2.20	0.92
7*	–	–	–	5.00	75.00	–	20.00	–	–

*Synthetic mixture of ternary system of MeOH-FAME-TG

TG as the limiting reactant and the forward and reverse reactions follow the second-order overall kinetics.[8] The γ may be estimated by using group distributions method based on UNIversal QUAsiChemical (UNIQUAC) thermodynamic model[18,24,25] with the aid from ChemCAD process flow sheet simulator. Once these values are known, Eqs. 45-49 can be solved for x_i^I and x_i^{II}. The calculated x_i^I and x_i^{II} values are then being substituted into Eq. 42. The iterations repeat until Eq. 42 is satisfied.

Membrane transport calculations

Once the bulk concentrations of $C_{b,i}^I$ obtained from the CPE calculation as shown in the section bulk concentrations at the feed side of the membrane reactor via chemical phase equilibrium (CPE) calculations are known, the transport equations of polarization layer and intramembrane filtration can be solved by means of numerical procedure. Because of the two-phase system (polarization layer and membrane) including a surface of discontinuity (phase interface), the numerical procedure requires continuity equations at appropriate boundary conditions. The equations of continuity expressed in terms of the concentration of component i (assuming no chemical reaction), take the form[12]

$$\frac{\partial(C)}{\partial t} = -\frac{\partial(N)}{\partial z}; \quad \text{for the polarization layer} \tag{50}$$

$$\frac{\partial(C)}{\partial t} = -\frac{\partial(N')}{\partial z}; \quad \text{for the intra}-\text{membrane} \tag{51}$$

Since the procedure is iterative, the initial estimate of the rejection of each solute, R_i^I and u^v are required. The initial guess of R_i^I can be estimated by assuming Poiseuille flow in the pores as[26]

$$R_i^I = 1 - \frac{C_{p,i}^I}{C_{b,i}^I} = 1 - 2\left(1 - \frac{r_{\text{solute}}}{r_{\text{pore}}}\right)^2 + \left(1 - \frac{r_{\text{solute}}}{r_{\text{pore}}}\right)^4 \tag{52}$$

where r_{pore} is the pore radius. The initial guess of u^v can be estimated from Eq. 7. Using the calculated values of the solute concentrations at the membrane-boundary layer interface ($z = 0$), the R_i^I and u^v are then calculated. The calculations of R_i^I and u^v will be terminated when the error between the initial guess and the calculated values are less than 5%.

Preliminary Experimental Analysis

This study investigated the effects of CPE on the separation efficiency of a membrane reactor at the preliminary stage to illustrate the importance of detailed modeling analysis. The transesterification experiment was first conducted in a batch reactor at difference catalyst concentrations and MeOH to TG molar ratios. The product in the reactor was then subjected to membrane separation at a constant temperature of 333 K, which was identical with the reaction temperature. In the real membrane reactor operation, the reaction and separation occurred simultaneously, which involved a dynamic change in the reaction and CPE at the feed side of the membrane reactor. This dynamic change was difficult to be measured experimentally. Therefore, to study the effects of CPE on the membrane separation, the reaction was isolated from the membrane separation by using a batch reactor. This allowed a constant equilibrated composition and phase at the feed side of the membrane reactor during the separation process. The detailed experimental procedures are illustrated in the following section.

Materials and Methods

Materials

The canola oil was purchased from Taiwan NJC Corp. Glycerin, monolein, diolein, triolein, butanetriol, tricaprin, methyl oleate, sodium hydroxide pellets and hydrochloric acid were supplied by Sigma-Aldrich Co. Methanol and n-heptane was of HPLC grade.

Batch reactor experiment

The transesterification of canola oil was performed in a 1 L batch reactor. The reaction temperature was controlled at 333 ± 0.2 K and agitation were provided by a stirrer controlled at a constant stirring speed of 100 rpm. A predetermined amount of canola oil was added to the reactor and heated to the desired temperature. The methanolic NaOH was then added to the base of the reactor carefully without agitation to prevent evaporation of the MeOH. The agitation was initialized, and the reaction was deemed to have started. The reaction was considered complete after 1 h of residence time and 12N hydrochloric acid was added to quench the reaction. Immediately, a sample was taken for concentration measurements of the total system. Subsequently, the product in the reactor was allowed to settle and separate into two phases at a constant temperature of 333 K. The volumes of both phases were measured, and samples from both phases were taken for concentration measurements. The errors involved in the system operation were calculated in term of overall mass balance analysis based on the measured concentrations and were maintained at <5%. Three experimental runs were carried out with different catalyst concentrations: 0.05, 0.1, 0.5 wt % based on TG at constant MeOH to TG molar ratio of 12:1. Three other experimental runs were carried out with different MeOH to TG molar ratios: 6:1, 18:1 and 24:1 at constant catalyst concentration of 0.1 wt %. All experimental runs summarized as in Table 1 were conducted

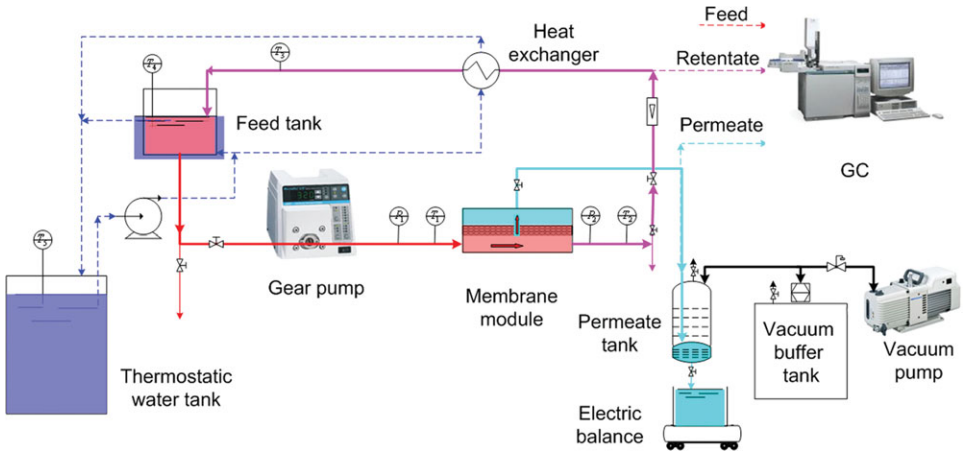

Figure 4. Schematic diagram for membrane system used for the biodiesel system.

[Color figure can be viewed in the online issue, which is available at wileyonlinelibrary.com.]

in triplicate with the standard deviations maintained below ±3%.

Membrane filtration experiment

The remaining portion of the reaction product was subjected to the ultrafiltration system as shown in Figure 4. A filtanium ceramic tubular membrane (TAMI, Nyons, France), which was made of titanium oxide was employed in the experiments. The membrane module had a molecular weights cut off (MWCO) of 300 kDa with a monolith configuration. The feed solution in a 0.0025m^3 thermostatic water bathed feed tank was circulated by using the 75211-30 digital gear pump (Cole-Parmer Instrument Co., USA) through the membrane module. The circulation flow rate was maintained at 0.018m^3/s with a constant pressure of 0.8 × 10^5kPa by the gear pump, whereas the permeate flux was obtained by measuring the time to collect a certain weight of fluid using the A&D electric balance (Tokyo, Japan). The feed flow rate and the transmembrane pressure were monitored and adjusted by flow control valves and the downstream gas vacuum pump (Tokyo, Japan). The operational variables were kept constant during the experiment, and the experiments were carried out by recycling only the retentate stream at 333 K so that the mobile phase (*Phase I*) and micelle (*Phase II*) can be collected in the permeate and feed tank, respectively at the end of the experiment. Each experimental run was conducted for 3,600 s and averaged flux data were collected. Permeate and retentate samples were taken at the end of the experiment for composition's analysis. After each run, the membrane was regenerated by using alkali-acid solution following the procedure recommended by the manufacturer. All the filtration experiments were conducted in triplicate with the standard deviations maintained below ±3%.

Analysis

The concentration measurements of each component were carried out by using gas chromatography (Agilent 6890N) with a flame ionization detector (FID) employing a DB-5HT capillary column (J&W Scientific) of 15 m length, 0.00032 m ID, 0.1 × 10^{-6} m film thickness with 5% phenyl and 95% methyl according to ASTM-D6584. A deactivated fused silica tubing (3 m × 0.00032 m) coated with syanophenylmethyl was used as the precolumn. Data collection and analysis were performed using Agilent Chemstation software, whereas 1,2,4-Butanetriol and tricaprin were used as the internal standard 1 and 2, respectively. A stock solution of n-heptane was added to the vial after the sample was silylated with N-methyl-N-trimethylsilyltrifluoracetamide (MSTFA). Samples were prepared by adding 4 mg of the samples to 20 × $10^{-6}m^3$ septa vials and one microliter was injected into the column. The calibration curves were generated by using the following standards: oleic acid (FAME), 1-monoolein (MG), 1,3-diolein (DG) and triolein (TG). The concentrations of the component in the sample were determined by the areas under the peaks in the chromatograms and the calibration curves.

Results and Discussion

Preliminary experimental analysis

The transesterification of canola oil in a batch reactor was conducted based on the operating conditions as shown in Table 1 (runs 1–6). On the other hand, to investigate the effect of a homogeneous system on the membrane separation efficiency, run 7 as shown in Table 1 was also incorporated into the study. In run 7, the transesterification experiment was not conducted but a synthetic mixture of MeOH-FAME-TG was used. The mixture composition was determined (as shown in Table 1) in a way that homogeneous mixture was obtained. The results as shown in Table 1 clearly demonstrate that the conversion of TG increased as the catalyst concentration increased which resulted in a higher FAME composition in the reaction mixtures. However, the conversion of TG decreased with the increase of MeOH to TG molar ratio from 12:1 to 24:1 at a constant catalyst concentration of 0.1 wt %. These observations were expected and in agreement with the observed trend of many researchers.[1,11,27] The results in Table 1 further confirmed that appropriate catalyst dosage and MeOH to TG molar ratio are needed to shift the reaction to the favorable path. However, it is important to note that for the MeOH to TG molar ratio of 12:1, 18:1 and 24:1, the MeOH phase became the continuous phase with lower viscosity. When the MeOH to TG molar ratio was reduced to 6:1, phase inversion occurred as the volume fraction of MeOH to TG ratio was less than 0.44. At this point, the TG phase of higher viscosity became the continuous phase whereas the MeOH phase became the dispersed phase (micelles).

For all the experimental runs of 1–6, the reaction mixture involved a heterogeneous system in which the mixtures

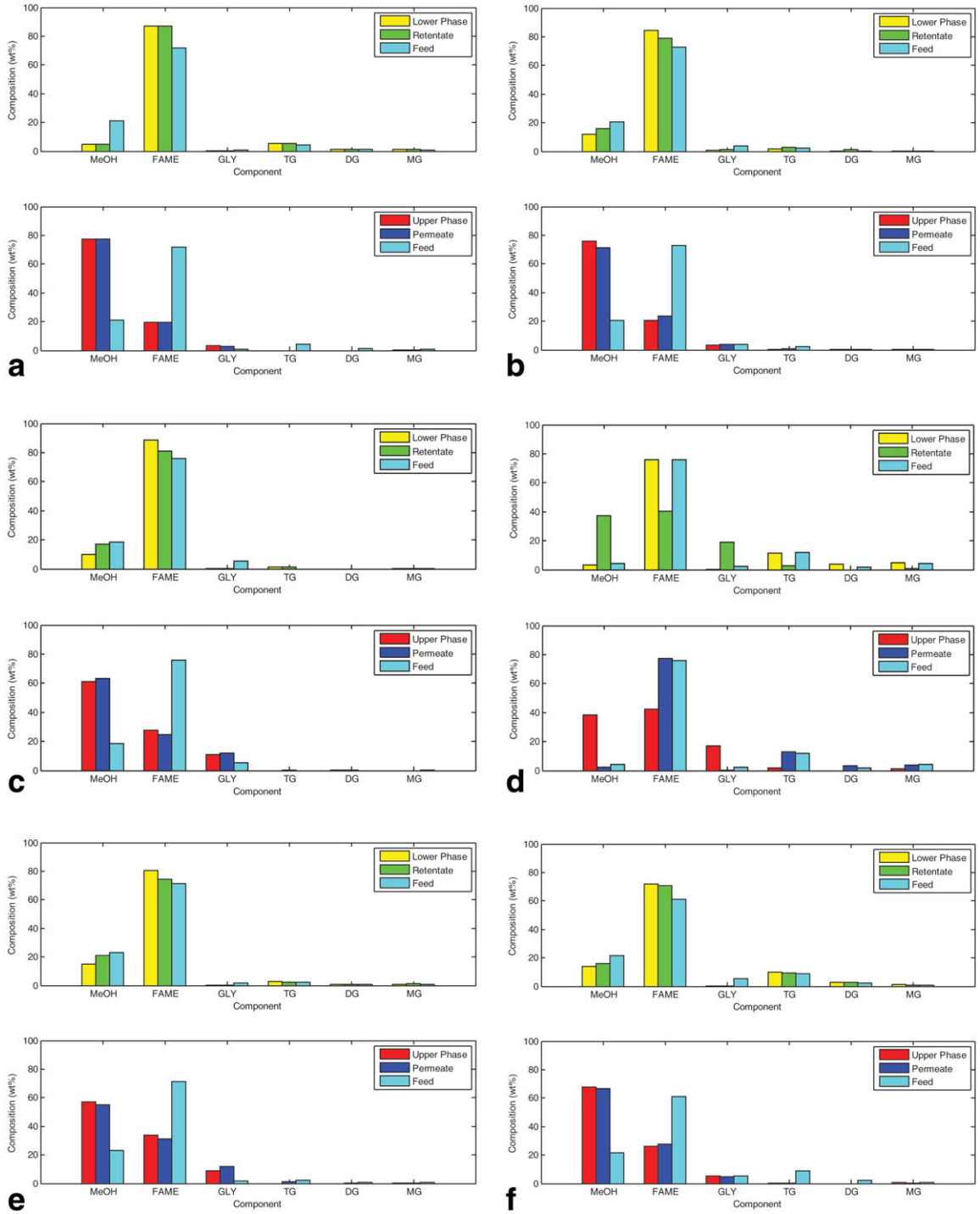

Figure 5. Upper and lower phase (CPE experiment) as well as permeate and retentate (membrane separation) compositions for run 1 (a), run 2 (b), run 3 (c), run 4 (d), run 5 (e), and run 6 (f).

Experimental conditions: varying catalyst concentrations of 0.05 wt % (run 1), 0.1 wt % (run 2) and 0.5 wt % (run 3) at constant MeOH to TG ratio of 12:1 for CPE; varyingMeOH to TG ratio of 6:1 (run 4), 18:1 (run 5) and 24:1 (run 6) at constant catalyst concentrations of 0.1 wt % for CPE; constant trans-membrane pressure of 0.8×10^5kPa at constant circulation rate of $0.018 m^3/s$ for membrane separation. [Color figure can be viewed in the online issue, which is available at wileyonlinelibrary.com.]

equilibrated into two liquid phases at a constant temperature of 333 K. The upper and lower phase compositions corresponding to each experimental run are shown in Figure 5. Although the upper phase consisted of a small amount of TG, DG and MG in all the experimental runs depending on the condition of CPE, the FAME concentrations were low as higher fraction of the FAME was solubilized in the lower phase, which contained higher TG, DG and MG concentrations at 333 K. In most of the experimental runs with MeOH to TG molar ratio of 12:1 and higher (especially runs 1, 3, 5 and 6), the TG in the upper phase was at negligible amounts as its concentrations were lower than the detectable limit of the gas chromatography (Agilent 6890N). The experimental run 4 with the MeOH to TG molar ratio of 6:1 consisted of

Table 2. Percentage of Deviation of Permeate from Upper Phase and Retentate from Lower Phase

	% of deviation of permeate from upper phase			% of deviation of retentate from lower phase		
Run	MEOH	FAME	Gly	MEOH	FAME	Gly
1	0.52	0.00	18.75	0.00	0.00	0.00
2	5.54	16.67	20.55	33.17	6.67	14.61
3	2.84	10.61	11.10	74.00	8.19	0.00
4	93.67	83.54	99.23	973	47.16	18720
5	3.50	6.38	33.71	40.00	7.48	0.00
6	1.77	7.51	14.70	14.71	1.39	0.00

the highest amount of TG in the upper phase (1.54%). This observation clearly demonstrates that the effects of CPE which were highly depending on the MeOH to TG molar ratio needed to be controlled carefully if the TG free upper phase was desired. This also signifies that if the membrane separation efficiency is highly depending on the formation of micelles, the TG free permeate can only be obtained when the CPE is controlled in such a way that the continuous phase must be free from TG, and the micelles should be large enough to be rejected by the membrane.

Figure 5 shows that the permeate stream and retentate compositions were closely related to the upper and lower phase compositions, respectively. This further confirmed the role of CPE and the formation of micelles in determining the separation efficiency of the membrane reactor. For the experimental runs of 1–3, the compositions of permeate and retentate closely followed the trend of the upper and lower phase compositions within a certain range of deviation as shown in Table 2. The deviation of compositions between the permeate stream and upper phase depicts that there was a small amount of micelles permeated through the membrane pores.

Furthermore, the average permeate flow rate undergone a drastic decrease from 1×10^{-6} m^3/s in run 1 to 0.45×10^{-6} m^3/s in run 2 as the catalyst concentration increased from 0.05 wt % to 0.1 wt %. The average permeate flow rate faced a further slight decrease to 0.35 mL/s when the catalyst concentration of 0.5 wt % (run 3) was used (not shown in any figure). This indicates that the ultra-low catalyst concentration should be recommended in the membrane reactor for biodiesel production to achieve a higher permeation flux. It is also worth highlighting that at ultra-low catalyst concentration of run 1, permeate stream and retentate compositions closely followed the upper and lower phase compositions, respectively as shown in Figure 5a with acceptable deviations (Table 2). This indicates that a high-rejection efficiency of micelles was achieved in run 1. The TG concentration in the permeate stream was also found to be negligible due to the negligible TG concentration in the corresponding upper phase. This result further supported the works done by Tremblay et al.[27] which recommended that ultra-low catalyst should be used.

Figure 5 shows that permeate and retentate compositions would only follow the upper and lower phase compositions if the MeOH to TG molar ratio was properly controlled due to the effects of CPE. As shown in Figure 5d of experimental run 4 and Table 2, permeate and retentate compositions deviated significantly from the upper and lower phase compositions, respectively. However, it is very interesting to find that the permeate composition was confirming with the trend of lower phase composition, whereas the retentate composition was following the upper phase composition. This observation depicts that the MeOH to TG molar ratio of 6:1 led to the TG phase to become the continuous phase due to phase inversion. As a result, the lower phase permeated through the pores of the membrane to give the highest TG concentration (12.86%) in the permeate stream among all the experimental runs. This also further confirmed that the formation of TG-rich micelles was crucial to ensure the quality of the permeate stream.

Figure 5e and f and Table 2 exhibit that permeate and retentate compositions closely followed the upper and lower phase composition within acceptable deviations, respectively. By comparing the percentage of deviation between runs 2, 5 and 6 as shown in Table 2, majority of the deviations between permeate and upper phase as well as retentate and lower phase decreased when the MeOH to TG ratio increased from 12:1 to 24:1. This shows that a higher rejection of micelles was achieved during the separation at high MeOH to TG molar ratio. The higher amount of MeOH led to a higher mobility of the continuous phase with lower viscosity during the permeation. At the meantime, the micelles concentration was also lower resulting in a higher rejection of micelles.

Many researchers[1,8,9,27,28] claimed that membrane reactor is an advanced technology to produce high purity of FAME which is free of bonded glycerides. In contradiction, other researcher[7] has proven that traces of DGs were detected when FAME concentration was above 25–35 wt %, but neither TG nor MG were found in the permeate stream. In another study,[9] significant TG was found in the permeate stream depending on the composition of the feed mixture. The inconsistent results obtained from all the aforementioned studies counter verified the results obtained in this study. The experimental results obtained in run 4 (Figure 5(d)) and run 7 (Figure 6) of this study clearly show that there were

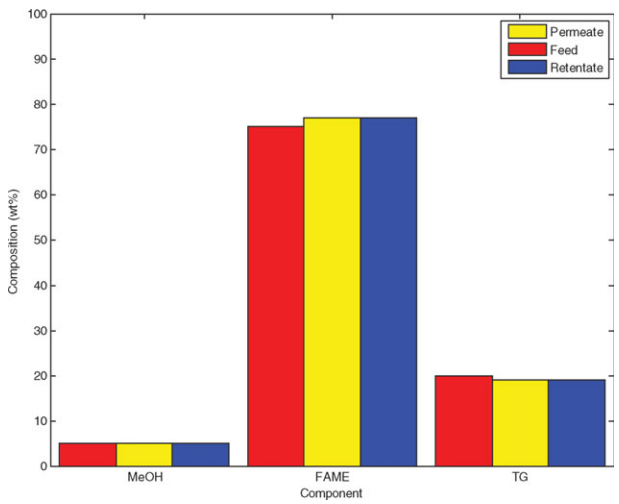

Figure 6. Feed mixture as well as permeate and retentate (membrane separation) compositions for run 7.

Experimental conditions: homogeneous feed mixture with the composition of 5 wt % MeOH, 75 wt % FAME and 20 wt % TG at constant trans-membrane pressure of 0.8×10^5kPa with constant circulation rate of $0.018 m^3/s$ for membrane separation. [Color figure can be viewed in the online issue, which is available at wileyonlinelibrary.com.]

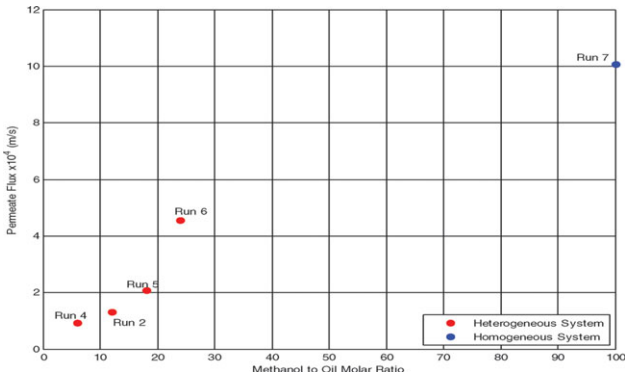

Figure 7. Effects of MeOH to TG molar ratio on permeate flow rate. Experimental conditions: varying MeOH to TG molar ratio at constant trans-membrane pressure of 0.8 × 10^5kPa with constant circulation rate of 0.018m^3/s for membrane separation.

[Color figure can be viewed in the online issue, which is available at wileyonlinelibrary.com.]

significant amount of glycerides (TG, DG and MG) in the permeate streams when phase inversion occurred or homogeneous reacting mixture was used. As shown in Figure 6, no separation was observed for experimental run 7 because permeate, retentate, and feed mixture compositions were identical due to the homogeneous state at the feed side of the membrane reactor. The observed results obtained in this study validated the significant of CPE and the knowledge of thermodynamic in ensuring the separation in a membrane reactor. The formation of micelles, whereas allowing the continuous phase to flow around them, whereas permeating through the membrane during simultaneous reaction and separation forms the most important requirement for efficient performance. The heterogeneity of the two liquid phases in the feed side of the membrane reactor needs to be controlled precisely to achieve the desired reaction and separation, and this can only be investigated through the modeling analysis.

Figure 7 shows that the average permeate flux increased with the increase of MeOH to TG molar ratio as the mobility of the permeating upper phase increased due to the increase of MeOH composition. The experimental run 4 with the MeOH to TG molar ratio of 6:1 achieved the lowest permeation flux due to the event of pore plugging by viscous TG-rich phase as the continuous phase. However, the permeation flux showed a significant increase as the MeOH to TG molar ratio increased from 18:1 (run 5) to 24:1 (run 6). This phenomenon shows the significant role of MeOH as the solvent in the continuous phase to carry the transesterification products across the membrane efficiently at minimal fouling due to the reduced viscosity. During the membrane separation of the homogeneous system in experimental run 7, the permeation flux increased 2.2 times higher than the permeation flux of run 6. As no separation occurred in experimental run 7, all components passed through the pores at higher permeation flux. These observations confirmed the findings of Cheng et al.[9] which highlighted the importance of LLE in influencing the permeation flux, and the permeate compositions.

Another important issue for the successful operation of the membrane reactor is the significant amount of FAME in the retentate stream as shown in Figure 5. Retentate is often being circulated back into the feed side of the membrane reactor due to its close loop operation.[27,28,29] This implies that if the FAME accumulates in the feed side of the membrane reactor, the increasing concentration of FAME will lead to a homogeneous condition which will not favor efficient reaction and separation besides facing the loss of the desired products. Nevertheless, experimental analysis on the feed side of the membrane reactor is unable to fully describe the reaction and separation behavior of the membrane reactor due to the close loop operation which is highly dynamic. As such, modeling analysis by using the mathematical model proposed in this study is indeed very important to investigate the behavior of membrane reactor for biodiesel production based on the fundamental of CPE, thermodynamic and multicomponent separations.

Model verification

The mathematical model developed in this study was verified by using the experimental data obtained from the preliminary experimental analysis. The model parameters determined based on the regression with the data obtained from membrane filtration experiment as described in the section membrane filtration experiment are shown in Table 3. The regression was done by minimizing the errors between the simulated values with the experimental values using the genetic algorithm as the optimization tool. The model calculation was initiated by the input of operating parameters and constants as well as initial guess of the solute rejections, and volumetric flux, due to the iterative procedure. The value of the only fitting parameter in the model regression, the equilibrium constant for membrane, was obtained once the errors were within 5%.

The estimated value of *Lp* as shown in Table 3 was higher than its typical value as reported in the literature.[30,31] This observation was expected as MEOH is less viscous than water, and, thus, the MEOH will permeate easily through the membrane than the pure water. As a result, the R_m value measured shows a lower value in an order of magnitude as compared to the literature values.[30,31] The values are highly depending on the cross-flow velocity, of the system and the values found were reasonable as compared to the reported values.[30,31] The $\varsigma = 1$ gave the best convergence in this study and similar observation was also found by Kerkhof.[12] The K_{eq}^{II} (as defined in Eqs. 22 and 34) values for TG, DG and MG were high as compared to other solutes. This observation indicates that the components of TG, DG and MG were more soluble in the lower phase (*Phase II*), and this phenomenon was further confirmed by Figure 5 in which most of the TG, DG and MG were found in the lower phase (*Phase II*). The K_{eq}^{m} (as defined in Eqs. 22 and 23) values for all the component were within the acceptable range as reported in the literature.[12] The value K_{eq}^{m} of 0.69 was

Table 3. Model Parameters used for Membrane Reactor Simulation

Parameters				Values		
L_p				3.2807 x 10^{-9} m/s.Pa		
σ				1		
R_m				6.7889 x 10^{11} m^{-1}		
u_t				0.0017 m/s		
k**				9.74 x 10^{-9} to 1.67 x 10^{-8} m/s		
i	**1**	**2**	**3**	**4**	**5**	**6**
K_{eq}^{II}	NA*	0.7613	6.4705	1220	600.4636	21.0390
K_{eq}^{m}	0.6785	0.5321	0.7631	1.2995	0.2561	0.1446

obtained for the transport of PEG-3400 in an ultrafiltration system with tubular module.[12] The slight deviation of the K_{eq}^{m} values with the literature can be explained by the different solute, solvent and membrane type involved. The low values of found in this study explained the insolubility of the solutes in the membrane matrix.

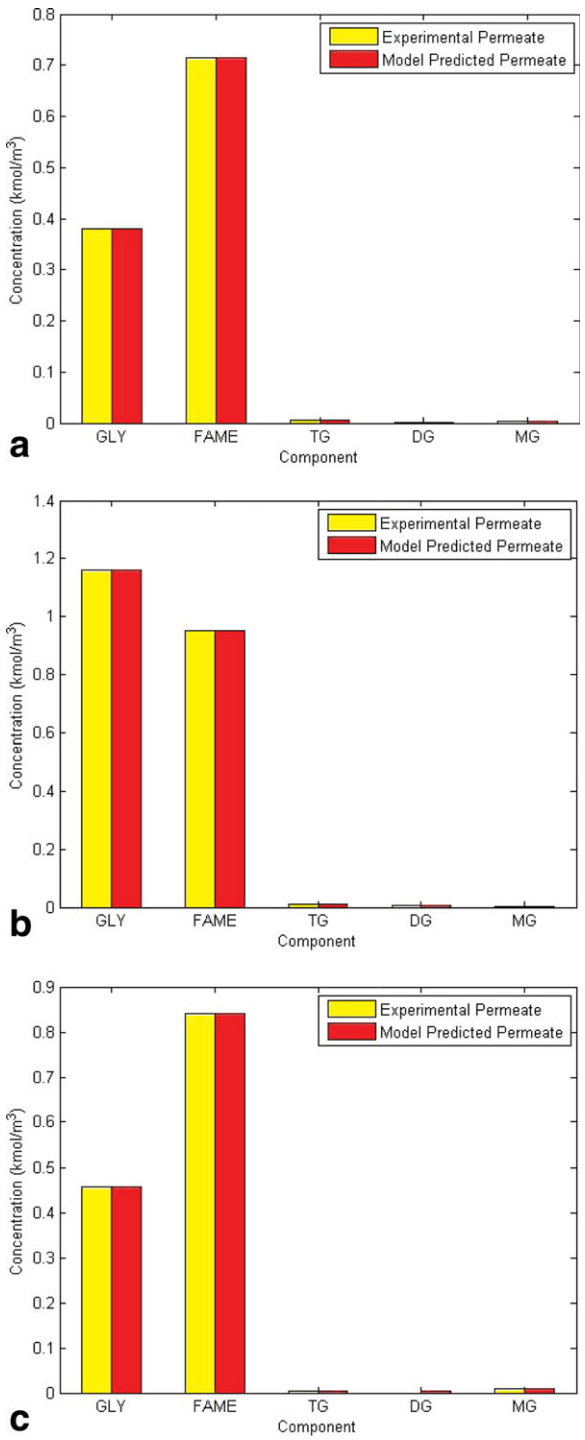

Figure 8. Mathematic model validation for canola oil transesterification reaction mixture as the feedstock (a) run 2, (b) run 5 and (c) run 6 at constant trans-membrane pressure of 0.8 × 10^5kPa and constant circulation rate of 0.018m^3/s for membrane separation.

[Color figure can be viewed in the online issue, which is available at wileyonlinelibrary.com.]

Table 4. The Experimental Rlux and Predicted Flux of the Membrane Reactor used in this Study

Experimental Run	Experimental Flux (m/s)	Predicted Flux (m/s)	Percentage of error (%)
2	1.33 x 10^{-04}	1.32 x 10^{-04}	0.13
5	2.07 x 10^{-04}	2.00 x 10^{-04}	3.42
6	4.56 x 10^{-04}	4.57 x 10^{-04}	0.12

The comparison of the experimental data and the model simulated data is shown in Figure 8 and Table 4. Figure 8a–c show permeate concentration of components Gly, FAME, TG, DG and MG at constant catalyst concentration of 0.1 wt % with different MeOH to TG ratio of 12:1 (run 2), 18:1 (run 5), and 24:1 (run 6), respectively. A good agreement between the experimental and simulated data was found in all the experimental runs with the coefficient of determination, R^2 of $\sim$ 1.0000 for the runs 2, 5 and 6 in Figure 8. The comparison between the experimental flux and the predicted flux as shown in Table 4 also indicates a good agreement with the percentage of error which was less that 5#. The good match between the model simulated results and the experimental results shows that the model can be used to accurately predict and investigate the performance of the membrane reactor for transesterification to produce biodiesel.

Conclusion

In this study, the mathematical model based on the modified Stefan-Maxwell model with the incorporation of the effects of CPE and thermodynamic suitable for biodiesel production using the membrane reactor was successfully developed and validated for the first time. The formation of micelles in the emulsion due to the heterogeneity of the reaction mixture and the presence of surfactants were the basis for the successful operation of a membrane reactor. Thus, the model was developed based on the assumption that under a controlled MeOH to TG molar ratio at the feed side of the membrane reactor, the MeOH-rich phase becomes the continuous phase, and transesterification occurs at the surface of micelles/oil droplets (TG-rich phase) formed due to efficient mixing. The continuous phase will then permeate through the membrane.

The preliminary experimental analysis confirmed the above assumption as efficient separation to produce permeate stream, which is free from bonded glycerides can only be achieved by maintaining the heterogeneity of the reacting mixtures at the correct MeOH to TG molar ratio. In addition, permeate compositions were closely related to the CPE of the system which emphasized the need of incorporating the CPE and thermodynamic effects into the modeling analysis. The preliminary experimental analysis also addressed the importance of modeling analysis to investigate the reactions and separations efficiency of the membrane reactor as well as the dynamic behavior of the close loop operation.

The model was successfully validated by using the experimental data obtained from the membrane filtration experiment with high-prediction capability. The model parameters also counter verify that the high solubility of TG, DG and MG in the lower phase (*Phase II*) were required to achieve bonded glycerides free permeate. Therefore, the model can be used for further detailed investigation on the performance of the membrane reactor for canola oil transesterification in biodiesel production.

Acknowledgments

The authors would like to gratefully acknowledge Chung-Yuan Christian University and The University of Nottingham for their financial support.

Notation

a = activity term
$\overline{a}$ = average activity term
B_o = permeability parameter
C = molar concentration
Ca = capillary number
Ca_{crit} = critical capillary number
D = Maxwell-Stefan diffusion coefficient
$\overline{D}$ = Fickian diffusion coefficient
D^o = infinite dilution diffusion coefficient
$[D]$ = Fickian molecular diffusion matrix
$[D]_{\text{turb}}$ = turbulence diffusivity matrix
D_{pore} = pore diameter
D_{solute} = solute diameter
D_{tube} = diameter of the tube
F = amount of the species
$[F]$ = convective part matrix
G = standard Gibbs free energy of formation
$[G]$ = generalized friction matrix
K = reaction equilibrium constants
$[K_{eq}]$ = equilibrium matrix
$[K_v]$ = convective friction matrix
k = phase equilibrium ratio
k = mass-transfer coefficient
k = constant valid for almost all substances and has a value of 2.1×10^{-7}
L_m = membrane thickness
L_{p} = hydraulic permeability constant
L_{tube} = length the tube
N = solute flux
n = number of solutes
n_{tube} = number of tubes per membrane module
M_j = molar mass of solvent
∇P = pressure gradient
ΔP_{flow} = driving force term
ΔP_{total} = total pressure difference of the system or trans membrane pressure
Q_F = volume feed flow rate
R = gas constant
R = rejection
Re = Reynolds number
$r_{\text{Miscelles}}$ = radius of the undeformed droplet
r_{pore} = pore radius
S = chemical species
Sc = Schmidt number
Sc_{turb} = turbulence Schmidt number
Sh = Sherwood number
$[S]$ = Fickian matrix inside the membrane
T = temperature
Tc = critical temperature of that substance i
u = velocity along the boundary layer
u_t = cross-flow velocity
u^v = volume-averaged velocity (or volumetric flux)
u^* = modified velocity
u^+ = dimensionless velocity
$\langle u_t \rangle$ = bulk velocity along the membrane
V = molar volume
$\overline{V}$ = specific molar volume
x = mole fraction
y = distance from surface in boundary layer
y^+ = dimensionless value of
z = distance coordinate perpendicular to the membrane surface
z = mole fraction in total system

Greek letters

γ = activity coefficient
$\overline{\gamma}$ = average activity coefficient
$\dot{\gamma}$ = shear rate
σ = osmostic reflection coefficient
$\dot{\sigma}$ = interfacial tension between the two fluids
$\dot{\sigma}$ = surface tension for a substance
v = kinematic viscosity
v_{turb} = turbulent kinematic viscosity
ρ = density
ρ = total mass concentration
η = viscosity
η_d = droplet fluid viscosity
η_c = continuous phase viscosity
$\dot{\eta}$ = dynamic viscosity of the mixture
Φ = volume fraction
Φ_j = association factor for the solvent
δ_{ij} = Kronecker delta
δ_{pol} = thickness of boundary layer
$\nabla_{T,P}\ \mu$ = chemical potential gradient
κ = fractional viscosity coefficient
ε = membrane porosity
τ = membrane tortuosity
f = fanning friction factor
α = mole fraction of *Phase I* in the system
ξ = extent of reaction
λ = viscosity ratio
β = stoichiometric coefficient
$\Delta\Pi$ = osmostic pressure difference across the membrane
Γ_c = thermodynamic factor

Subscripts

b = bulk condition
in = initial
i, j = individual component/solute
j = reaction indices
m = inside the membrane
out = final
p = permeate
t = total
DG = diglyceride
$FAME$ = fatty acid methyl ester
Gly = glycerol
$MEOH$ = methanol
MG = monoglyceride
TG = triglyceride

Superscripts

I = *phase I*
II = *phase II*
m = membrane

Matrix notation

$[\ ]$ = square matrix
$[\ ]^{-1}$ = inverted matrix
$()$ = component vector

Literature Cited

1. Dubé MA, Tremblay AY, Liu J.Biodiesel production using a membrane reactor. *Bioresour Technol*. 2007;98:639–647.
2. Zhou H, Lu H, Liang B.Solubility of multicomponent systems in the biodiesel production by transesterification of jatropha curcas l. oil with methanol. *J Chem Eng Data*. 2006;51(3):1130–1135.
3. Noureddini H, Zhu D.Kinetics of transesterification of soybean oil. *J Am Oil Chem Soc*. 1997;74(11):1457–1463.
4. Boocock DGB, Konar SK, Mao V, Sidi H.Fast one-phase oil-rich processes for the preparation of vegetable oil methyl esters. *Biomass Bioenergy*. 1996;11(1):43–50.
5. Saka S, Kusdiana D.Biodiesel fuel from rapeseed oil as prepared in supercritical methanol. *Fuel*. 2001;80(2):225–231.
6. Knothe G, Krahl J, Van Gerpen J. *The biodiesel handbook*. Champaign, IL: AOCS Press; 2005.
7. Cao P, Tremblay AY, Dubé MA, Morse K.Effect of membrane pore size on the performance of a membrane reactor for biodiesel production. *Ind Eng Chem Res*. 2007;46(1):52–58.
8. Cao P, Tremblay AY, Dube MA.Kinetics of canola oil transesterification in a membrane reactor. *Ind Eng Chem Res*. 2009;48(5):2533–2541.

9. Cheng LH, Cheng YF, Yen SY, Chen J.Ultrafiltration of triglyceride from biodiesel using the phase diagram of oil-FAME-MeOH. *J Membr Sci*. 2009;330(1–2):156–165.
10. Zhou W, Boocock DGB.Phase behavior of the base-catalyzed transesterification of soybean oil. *JAOCS*. 2006;83(12):1041–1045.
11. Freedman B, Pryde EH, Mounts TL.Variables affecting the yields of fatty esters from transesterified vegetable oils. *J Am Oil Chem Soc*. 1984;61(10):1638–1643.
12. Kerkhof PJAM.A modified Maxwell-Stefan model for transport through inert membranes: the binary friction model. *Chem Eng J*. 1996;64:319–343.
13. Oers CW, Vorstman MAG, Hout RVD, Kerkhof PJAM.The influence of thermodynamic activity on the solute rejection in multicomponent systems. *J Membr Sci*. 1997;136:71–87.
14. DeRoussela P, Khakharb DV, Ottinoa JM.Mixing of viscous immiscible liquids. Part 2: Overemulsification - interpretation and use. *Chem Eng Sci*. 2001;56:5531–5537.
15. Pal R. *Rheology of Particulate Dispersions and Composites. Surfactant Science Series*. USA, CRC Press, Taylor and Francis Group; 2006.
16. Krishna R.A simplified procedure for the solution of the dusty gas model equations for steady-state transport in non-reacting systems. *Chem Eng J*. 1987;35:75–81.
17. Ahmad AL, Chong MF, Bhatia S.Mathematical modeling and simulation of the multiple solutes system for nanofiltration process. *J Membr Sci*. 2005;253:103–115.
18. Taylor R, Krishna R. *Multicomponent mass transfer*. New York: Wiley-IEEE, 1993.
19. Wijmans JG, Baker RW.The solution-diffusion model: a review. *J Membr Sci*. 1995;107:1–21.
20. Sieder EN, Tate GE.Heat transfer and pressure drop of liquids in tubes. *Ind Eng Chem*. 1936;28(12):1429–1435.
21. Ho RM, Wu CH, Su AC.Morphology of plastic/rubber blends. *Polym Eng Sci*. 1990;30(9):511–518.
22. Fogler HS. *Elements of Chemical Reaction Engineering*. 3rd ed. New Jersey: Prentice Hall PTR; 1999.
23. Sanderson RV, Chien HHY.simultaneous chemical and phase equilibrium calculation. *Ind Eng Chem Process Des Dev*. 1973;12(1):81–85.
24. Poling BE, Prausnitz JM, O'Connell JP. *Properties of Gases and Liquids*. New York: McGraw-Hill; 2001.
25. Singh MK, Banerjee T, Khanna A.Genetic algorithm to estimate interaction parameters of multicomponent systems for liquid-liquid equilibria. *Comput Chem Eng*. 2005;29:1712–1719.
26. Sarbolouki MN, Miller AIF.On pore flow models for reverse osmosis desalination. *Desalination*. 1973;12:343–359.
27. Tremblay AY, Cao Peigang, Dubé MA.Biodiesel production using ultralow catalyst concentrations. *Energy Fuels*. 2008;22(4):2748–2755.
28. Cao P, Dubé MA, Tremblay AY.High-purity fatty acid methyl ester production from canola, soybean, palm, and yellow grease lipids by means of a membrane reactor. *Biomass Bioenergy*. 2008;32(11):1028–1036.
29. Cao P, Dubé MA, Tremblay AY.Methanol recycling in the production of biodiesel in a membrane reactor. *Fuel*. 2008;87:825–833.
30. Mehta A, Zydney AL.Permeability and selectivity analysis for ultrafiltration membranes. *J Membr Sci*. 2005;249:245–249.
31. Ahmad AL, Chong MF, Bhatia S.Ultrafiltration modeling of multiple solutes system for continuous cross-flow process. *Chem Eng Sci*. 2006;61:5057–5069.

Appendix A

The differentiation of with respect to molar concentration in the elements of the thermodynamic matrix, $[\Gamma_c]$ which is valid for Wilson, NRTL and UNIQUAC thermodynamic models is given as[18]

$$\frac{\partial \ln \gamma_i}{\partial C_j} = \frac{1}{C_t}\left(Q_{c,ij} - Q_{c,in}\right) \tag{A1}$$

The dimensionless excess Gibbs energy, $Q_{c,ij}$ for UNIQUAC model is given as

$$Q_{c,ij} = Q^c_{c,ij} + Q^r_{c,ij} \tag{A2}$$

where

$$\begin{aligned} Q^c_{c,ij} &= -\frac{r_i}{r} - \frac{r_j}{r} + \left(\frac{r_i r_j}{r^2}\right)\chi - \frac{z}{2}q\left(\frac{r_j}{r} - \frac{q_j}{q}\right)\left(\frac{r_i}{r} - \frac{q_i}{q}\right) \\ Q^r_{c,ij} &= q_i q_j\left(1 - \varepsilon_{ij} - \varepsilon_{ji} + \sum_{k=1}^{n}\theta_k \varepsilon_{ik}\varepsilon_{jk}\right)/q \end{aligned} \tag{A3}$$

The coordination number, term z is 10, q_i is relative surface area of pure component i and r_i is relative volume of pure component i. The term $Q_{c,ij}$ is symmetric and other variables are given as:

$$r = \sum_{i=1}^{n} x_i r_i \tag{A4}$$

$$q = \sum_{i=1}^{n} x_i q_i \tag{A5}$$

$$\chi = \sum_{j=1}^{n} x_j \tag{A6}$$

$$\theta_i = \frac{x_i q_i}{q} \tag{A7}$$

$$\tau_{ij} = \exp\left[-\frac{a_{ij}}{RT}\right] \tag{A8}$$

$$S_i = \sum_{j=1}^{n} \theta_j \tau_{ji} \tag{A9}$$

$$\varepsilon_{ik} = \frac{\tau_{ik}}{S_k} \tag{A10}$$

The τ_{ij} is UNIQUAC empirical parameter, whereby $\tau_{ii} =$ 1and a_{ij} is binary interaction energy parameter estimated from experimental data.

Manuscript received July 14, 2011, revision received Jan. 27, 2012, and final revision received Mar. 23, 2012.